The effects of early Cambrian metamorphism in western Dronning Maud Land, East Antarctica: a carbon and oxygen isotope study of fluid–rock interaction in the Sverdrupfjella Group

WARREN P. JOHNSTONE & CHRIS HARRIS

Department of Geological Sciences, University of Cape Town, Rondebosch 7700, Republic of South Africa (email: charris@geology.uct.ac.za)

Abstract: The Sverdrupfjella Group in western Dronning Maud Land is a 1200 to 900 Ma orogenic belt that experienced a thermal overprint in the early Cambrian. Evidence for distinct episodes of fluid–rock interaction is found in calc-silicate rocks, veins and retrograde mineral assemblages. A sequence of altered but undeformed basalts exhibit extreme ^{18}O depletion ($\delta^{18}O$ as low as −1.8‰) apparently due to interaction with meteoric water during regional (possibly early Cambrian) metamorphism. In the central Kirwanveggen, metasomatic calc-silicates, and retrograde mineral assemblages are associated with late high-strain zones of probable Cambrian age. The former have $\delta^{13}C$ values which overlap those of massive metacarbonate units 150 km to the NE, and imply regional scale movement of fluids. The latter record ^{18}O depletion relative to unretrogressed equivalent rocks and suggest interaction with externally derived fluids.

The understanding of crustal evolution in many parts of Gondwana is complicated by the difficulty in distinguishing the effects of *c.* 500 Ma overprinting of *c.* 1000 Ma orogenic belts. The Mesoproterozoic high-grade Circum East Antarctic Mobile Belt (Yoshida 1992) has been variably affected by an early Palaeozoic (550–500 Ma) metamorphic event (Groenewald 1991; Grantham *et al.* 1995; Groenewald *et al.* 1995; Krynauw 1996). Geochronological studies in central and eastern Dronning Maud Land (Fig. 1) show that this early Cambrian high-grade metamorphism was associated with magmatism and deformation, and reached granulite facies conditions in places (e.g. Shiraishi *et al.* 1992; Dirks *et al.* 1993; Fitzsimons 1998). The Maud Belt of western Dronning Maud Land is the westernmost part of the Circum East Antarctic Mobile Belt, where the effects of the Cambrian metamorphism are least well developed (Fig. 1). Although early Cambrian Rb–Sr and K–Ar cooling ages are recorded in the Maud Belt (e.g. Moyes *et al.* 1993; Krynauw 1996), these appear to be associated with a greenschist–amphibolite facies thermal overprint accompanying the emplacement of granitoid bodies. Cambrian deformation appears to be re-stricted largely to mylonite zones of limited development, which contain hydrous mineral assemblages and thus record the passage of syn- and possibly post-deformation fluids. In terms of understanding the overall effects of Cambrian metamorphism, it is important to determine to what extent the thermal overprint recorded in the Cambrian was accompanied by pervasive fluid–rock interaction associated with the developments of the mylonite zones. A study of the fluid–rock interaction enables an assessment to be made of the extent of crustal 'reworking' in the absence of significant structural features.

In the Maud Belt, as in the case of many other metamorphic terranes, there is abundant field evidence for fluid–rock interaction, in the form of veins, hydrous retrograde mineral assemblages, and metasomatic rocks. However, when the terrane has undergone a complex geological history involving multiple episodes of deformation and metamorphism, it can be difficult to ascertain when fluid–rock interaction occurred and whether it resulted from a single or multiple periods of metamorphism. This is exacerbated by the problems of dating fluid–rock interaction and it may not be easy to determine the relationship between different metamorphic and/or deformation episodes, and different episodes of fluid–rock interaction.

In this study oxygen and carbon isotopes have been used to investigate the nature and extent of these episodes of fluid–rock interaction recorded in the Sverdrupfjella Group. Stable isotopes alone cannot provide any age constraints, but in combination with previously published accounts of the crustal evolution of the area (Grantham

From: MILLER, J. A., HOLDSWORTH, R. E., BUICK, I. S. & HAND, M. (eds) *Continental Reactivation and Reworking*. Geological Society, London, Special Publications, **184**, 381–394. 1-86239-080-0/01/$15.00

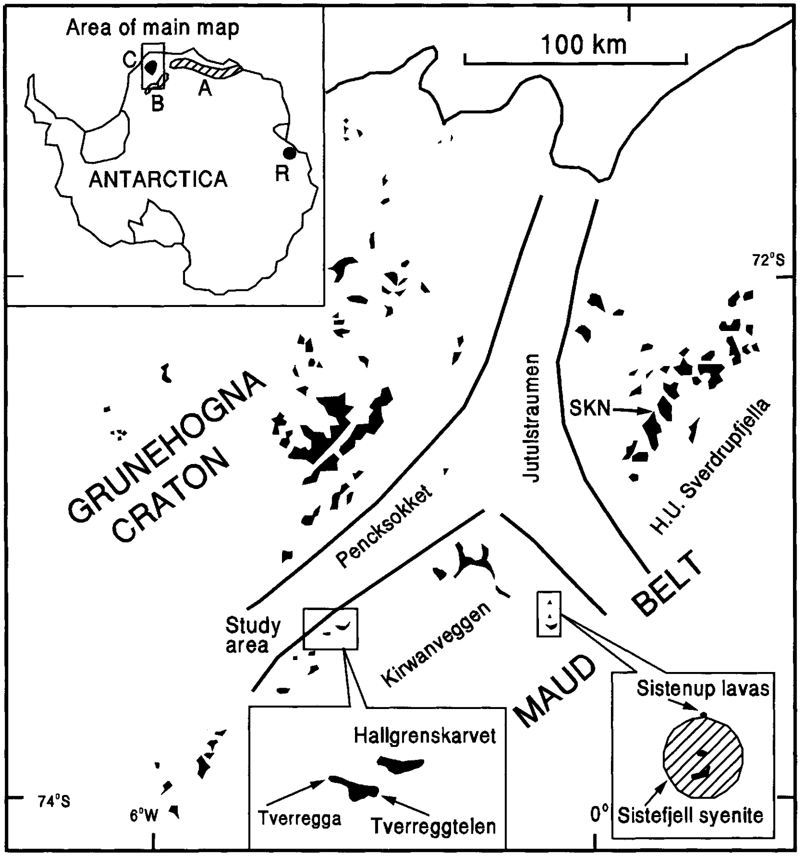

Fig. 1. Regional Geological Map of western Dronning Maud Land, East Antarctica. The Grunehogna Craton is separated from the Maud Belt by the Jutulstraumen–Pencksokket glaciers. The metacarbonate samples (WJS1–6) from the Fuglefjellet Formation were collected at Skarsnuten (SKN) in the H.U. Sverdrupfjella. The inset geological map of Antarctica shows the position of parts of the East Antarctic Mobile Belt which were affected by high-grade Cambrian metamorphism (A); those parts of the mobile belt which were not affected by Cambrian high-grade metamorphism (B); the Grunehogna Craton (C); and the location of the Rauer Group (R). The shape of the Mesozoic Sistefjell syenite is interpreted from aeromagnetic data (Corner 1994). Note that H.U. Sverdrupfjella refers to the mountain range to the west of the Jutulstraumen Glacier; the Sverdrupfjella Group comprises rocks from both the H.U. Sverdrupfjella and the Kirwanveggen montain range to the east of the Jutulstraumen.

et al. 1995; Groenewald *et al.* 1995), can be used to construct the extent of fluid–rock interaction during the complex metamorphic history of western Dronning Maud Land. Stable isotope studies have been successfully applied to similar aged 'Pan-African' reworking of older high-grade metamorphic rocks of Madagascar by Pili *et al.* (1997).

Regional geological setting

Western Dronning Maud Land (Fig. 1) is characterized by two areas with distinctly different geological histories. To the west of the Jutulstraumen–Penksokket glaciers (Fig. 1), the major rock types are relatively undeformed sedimentary sequences and magmatic rocks of uncertain age (but >1000 Ma) that overlie Archaean granite (Groenewald *et al.* 1995). This western area has been termed the Grunehogna Craton and is interpreted as a fragment of the Kalahari Craton (Wolmarans & Kent 1982; Krynauw 1996). To the east of the Jutulstraumen–Penksokket glaciers, high-grade metamorphic rocks make up the Sverdrupfjella Group (Roots 1969; Hjelle 1974). This terrane has been termed the Maud Belt (Groenewald *et al.* 1995) and it forms part of the Mesoproterozoic Circum East Antarctic Mobile Belt (Yoshida 1992).

Most of this paper concerns the amphibolite to granulite facies rocks of the Sverdrupfjella Group in the Kirwanveggen mountain range in the Maud Belt. The metamorphic history of these rocks are summarized by Grantham *et al.* (1995) and Groenewald *et al.* (1995). The earliest metamorphism involved high-grade conditions (12–15 kbar, 750°C) during prograde metamorphism between 1200 Ma and 900 Ma followed by decompression and thermal relaxation (8 kbar, 850°C). These conditions are attributed by Groenewald *et al.* (1995) to continental collision (the 'Maud Orogeny') involving deep burial with an elevated geotherm of a marginal basin. The Cambrian metamorphism reached amphibolite facies conditions (5–6 kbar, 600°C). This later orogenic episode has been correlated with 'Pan African' orogenesis (Grantham *et al.* 1995; Krynauw 1996) and resulted in tectonic inversion of the metamorphic profile by thrusting, followed by rapid uplift and exhumation (Groenewald *et al.* 1995). Apart from Mesozoic intrusions, the only undeformed rocks in the area are the late Precambrian Sistenup lavas (Ravich & Solov'ev 1969). These lavas are pervasively altered to amphibolite facies assemblages that, because of the lack of associated deformation, may be Cambrian in age.

Petrography

Sistenup lavas

The Sistenup lavas (Fig. 1) are considered to be correlatives of the Precambrian Richtersflya Supergroup, which is exposed on the Grunehogna Craton (Ravich & Solov'ev 1969). The lavas are dominantly basaltic with minor evolved types (SiO_2 up to 66 wt.%), and it is important to note that they are undeformed except that flows dip at about 30°S. They are highly altered with hornblende as the dominant secondary mineral. Some samples contain abundant large (up to 3 cm long) laths of plagioclase that in thin section appear comparatively unaltered. The plagioclase exhibits well-developed igneous zoning and is set in a groundmass of amphibole. The abundance of secondary hornblende rather than chlorite and epidote, and the comparative stability of plagioclase, is evidence of alteration at elevated temperatures. The temperature at which hornblende rather than chlorite forms in mafic systems is strongly dependent on oxygen fugacity, PH_2O and Ptotal (e.g. Apted & Liou 1983), but is probably at least 450°C. Experimental work by Apted & Liou (1983) and Moody *et al.* (1983) showed that the relict calcic plagioclase persists up to 600°C at QFM buffer conditions of 7 kbar (PH_2O = Ptotal). Although the Sistenup lavas are exposed only at the contact with a Mesozoic syenite intrusion, it is suggested that the amphibole resulted from much earlier fluid–rock interaction (see below).

Calc silicates and metacarbonates

Regionally extensive units (>300 m thick and 5 km strike length) consisting of marbles, and quartzofeldspathic and calc-silicate gneisses are exposed in the H.U. Sverdrupfjella mountain range (Fig. 1) where they collectively make up the Fuglefjellet Formation (Hjella 1974; Grantham *et al.* 1995; Groenewald *et al.* 1995). According to Groenewald *et al.* (1995), these carbonates represent a shallow-marine sequence. Although they are best preserved at Fuglefjellet, substantial thicknesses are also exposed at Skarsnuten further south (Fig. 1), where a 200 m high cliff reveals a package of alternating bands of sparry calcite (up to 3 m thick) and quartzofeldspathic gneiss punctuated by strings of boudinaged calc-silicate gneiss.

In contrast, in the central Kirwanveggen (Fig. 1) calc-silicate mineral assemblages are rare. Scattered calc-silicate boudins in quartz–feldspar–biotite gneisses (Fig. 2a) conform to the early regional fabric and are hosted in an extensive horizon that forms part of the Tverregga Banded Gneiss described by Grantham *et al.* (1995). Individual boudins range from 5 to 20 cm in size, are ellipsoidal in shape with the long axis parallel to the mineral stretching lineation within the plane of the foliation (Fig. 2a). They show a mineral zonation from cores which are relatively rich in mafic minerals and comprise quartz–K-feldspar–plagioclase–diopside–hornblende–epidote with minor calcite and sphene to more felsic rims of plagioclase–quartz–K-feldspar with minor calcite. A second type of calc-silicate rock occurs in the form of a metasomatic alteration body at Tverreggtelen. This body extends for at least 150 m along strike and is hosted within a late shear zone (Fig. 2b). The metasomatic paragenesis comprises calcite–diopside with variable amounts of hornblende–actinolite ± chlorite ± serpentinite ± tremolite ± talc ± epidote. The body consists of a hornblende and diopside-rich core surrounded by an outer zone consisting of calcite–quartz–diopside–tremolite–talc–sphene, with a rim of quartz–calcite–hornblende–talc–serpentinite–actinolite and diopside.

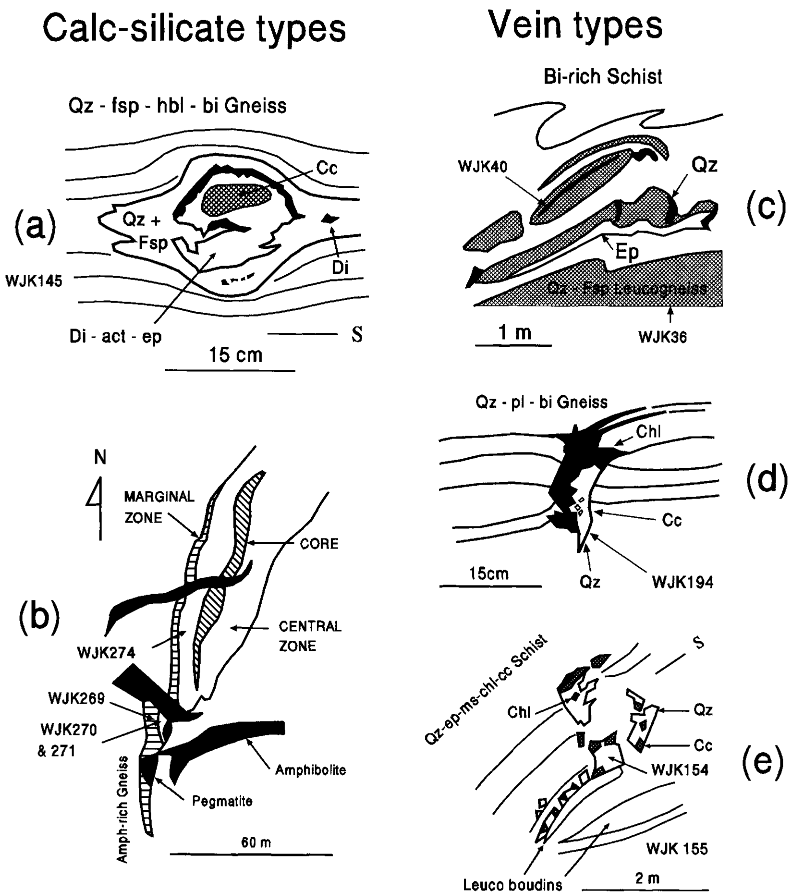

Fig. 2. Calc-silicate rocks and vein types sampled in the central Kirwanveggen. (**a**) Field sketch of a single zoned calc-silicate boudin. *S* denotes the foliation of the host gneiss, the orientation of the line is parallel to the direction of the mineral stretching lineation within the plane of the foliation. (**b**) Sketch map of the metasomatic calc-silicate body at Tverreggtelen. The core comprises hbl–di; the central zone comprises cc–qz–di–trem–tc–sph; and the marginal zone comprises qz–cc–hbl–tc–serp–act–di. Mineral abbreviations: act, actinolite; bi, biotite; cc, calcite; di, diopside; ep, epidote; fsp, feldspar; hbl, hornblende; serp, serpentinite; sph, sphene; tc, talc; trem, tremolite; qz, quartz. (**c**–**e**) Vein types in the central Kirwanveggen (**c**) synfolial, (**d**) boudin-eye and (**e**) discordant. *S* denotes the foliation of the host gneiss.

Veins

Veins are ubiquitous throughout the central Kirwanveggen and attest to the presence of fluids during the evolution of this part of the Maud Belt. However, the scale of fluid-flow during vein formation remains a subject of considerable debate (e.g. Gray *et al.* 1991; Henry *et al.* 1996) with possible end-member behaviour ranging from percolation of large volumes of fluid on the scale of an orogenic belt, to closed-system behaviour on the scale of a geological formation, where fluid occupies pore spaces and is essentially static. In the central Kirwanveggen, the majority of veins consist of quartz, a minority of which also contain calcite. Some of the veins show a more complex mineralogy, e.g. quartz–chlorite–calcite ± feldspar ± biotite and quartz–hornblende–feldspar ± epidote ± calcite. The veins can be classified as: synfolial, boudin-eye and discordant types according to their form and structural disposition in the field (Fig. 2c, d and e). Synfolial veins regularly indicate a sense of shear while boudin-eye veins fill dilational sites within the boudinaged fabric. These two vein types are likely to have been formed by pressure solution processes during fabric development. The discordant veins show a variety of geometrical forms, these include irregular vug-filling and fracture-filling varieties as well as tension gash arrays. The process by which discordant veins form is distinct from that which is responsible for the formation of synfolial veins because they reflect more brittle conditions. The synfolial and boudin-eye vein types precipitated from a fluid phase present during regional fabric development whereas the discordant veins are probably the result of later fluid–rock interaction at a shallower level in the crust.

Hydrous retrograde mineral assemblages

Greenschist facies overprinting of upper amphibolite and granulite facies mineral assemblages is widespread in the central Kirwanveggen (e.g. Krynauw 1996). Some of the best examples of this overprinting occur in banded gneisses at Halgrenskarvet and Tverregga (Fig. 1). These rocks display a variable degree of hydrous retrogression characterized by retrograde assemblages of biotite, chlorite and epidote with lesser amounts of sericite, titanite and calcite. The retrograde mineral assemblages are associated with high strain zones within the banded gneiss and often exhibit mylonitic textures. These high strain zones define the moderately SE-dipping regional planar fabric of the central Kirwan-veggen. Lineations are generally down-dip, and field criteria indicate a top-to-the-north-west sense of shear. Grantham *et al.* (1995) described retrogressed diopside–epidote–plagioclase calc silicate gneiss, chlorite phyllite, actinolite–epidote–chlorite–calcite schist and tremolite–serpentine schist components from what they call the Tverregga Banded Gneiss. Similar assemblages are observed around the margins of an intrusive leucogranite at nearby Tverreggtelen, and within a thick sequence of banded gneisses at Hallgrenskarvet (Fig. 1). These zones consist of three distinctive lithological components (Fig. 2b), namely quartz–chlorite–epidote–biotite schist, quartz–K-feldspar–plagioclase–sericite–chlorite schist, and quartz–epidote–muscovite–chlorite–calcite–titanite schist. Quartzo–feldspathic gneisses in these zones have epidote and biotite as major phases whereas magnetite, titanite, apatite and allanite are common accessory phases in most of the samples from this area. On the basis of the similarity of these features with those that cut 500 Ma mafic dykes in the Heimefrontfella to the southwest, Grantham *et al.* (1995, pp. 217–218) concluded that the high-strain zones and the associated hydrous retrogression are Cambrian in age.

Analytical techniques

The majority of the analytical data reported in this paper were produced at the University of Cape Town (UCT). Some of the silicate $\delta^{18}O$ values were obtained at Monash University. Mineral separates were obtained by a combination of hand-picking and magnetic separation. Oxygen isotope ratios determined in both laboratories were obtained by conventional methods using ClF_3 as the oxidizing reagent (Borthwick & Harmon 1982). Data are reported in δ notation where $\delta^{18}O = (R_{sample}/R_{standard} - 1) * 1000$ and $R = {}^{18}O/{}^{16}O$. At UCT, a quartz standard (MQ) calibrated against NBS-28 was analysed in duplicate with each run of eight samples and used to convert the raw data to the SMOW scale using the value of 9.64‰ for NBS-28 recommended by Coplen *et al.* (1983). The average observed difference between MQ duplicates during the course of this work was 0.13‰. Further details of the methods used for the extraction of oxygen from silicates at UCT are given by Vennemann & Smith (1990) and Harris & Erlank (1992). Standards run at Monash gave $\delta^{18}O$ values within 0.2‰ of their accepted values and the long-term average $\delta^{18}O$ value of NBS-28 is 9.58 ± 0.12‰.

Carbon and oxygen isotope ratios of calcite were obtained at UCT according to the method of McCrea (1950). A fractionation factor of 1.01025 was used to correct the $\delta^{18}O$ value of the acid liberated CO_2 to that of calcite. The $\delta^{18}O$ and $\delta^{13}C$ values are reported with respect to the SMOW and PDB reference standards, respectively, to which they were calibrated using an internal carbonate standard calibrated using NBS-19 ($\delta^{18}O$, 28.64‰; $\delta^{13}C$, 1.95‰).

Results

Sistenup lavas

The Sistenup lavas show a range in whole-rock $\delta^{18}O$ values from −1.8 to +4.4‰ (Table 1). The very low values occur in both aphyric and plagioclase–phyric varieties of the basalt. In two highly porphyritic samples where plagioclase–whole-rock pairs were analysed, the plagioclase and whole-rock $\delta^{18}O$ values were of −0.1 and −0.6‰, and 4.7 and 4.4‰ respectively. The small difference between plagioclase and whole-rock $\delta^{18}O$ values suggests approximate oxygen isotope equilibrium between phenocrysts and groundmass. There is no systematic variation of whole-rock $\delta^{18}O$ value with distance from the intrusion and/or stratigraphic height at Sistenup.

Table 1. *Whole-rock oxygen isotope data for retrogressed rocks*

Sample	Rock type	$\delta^{18}O$	Sample	Rock type	$\delta^{18}O$
Tverregga			Hallgrenskarvet		
WJK155	qz–ep–chl–ms schist	5.4	WJK20	qz–fsp–ms–bi gneiss	3.5
WJK156	qz–fsp–ser–chl schist	12.0	WJK21	qz–fsp–ms–bi gneiss	4.0
WJK159	qz–ep–bi gneiss	8.7	WJK22	qz–fsp–ms–bi gneiss	5.3
WJK160	qz–ksp–bi–ms gneiss	9.3	WJK23	qz–fsp–ms–bi gneiss	4.1
WJK180	qz–ksp–ep leucosome	10.4	WJK24	qz–fsp–ms–bi gneiss	6.3
WJK193	qz–pl–bi–ep gneiss	4.9	WJK36	qz–pl–ksp gneiss	7.7
WJK196	qz–pl–bi gneiss	7.8	WJK37	qz–bi–ep schist	6.8
WJK199	qz–fsp pegmatite	8.8	WJK50	qz–fsp–ms–bi gneiss	6.3
WJK200	qz–pl–bi gneiss	7.9	WJK68	qz–fsp–bi gneiss	10.5
WJK201	qz–ksp–bi–ep agmatite	7.5	WJK74	qz–fsp–bi schist	4.2
WJK202	qz–fsp–bi gneiss	10.2	WJK80	qz–ksp–pl–ms gneiss	9.3
WJK205	qz–ksp–bi gneiss	7.8	WJK82	qz–fsp–hbl–bi schist	6.3
WJK207	qz–ksp–bi–ep agmatite	8.2	WJK85	qz–fsp–bi schist	4.6
WJK208	qz–fsp–bi gneiss	8.2	WJK95	qz–pl–bi schist	6.1
WJK209	qz ultramylonite	9.7	WJK97	qz–pl–bi schist	8.0
WJK210	qz–fsp–bi gneiss	9.1	WJK20	qz–fsp–ms–bi gneiss	3.5
WJK211	qz–fsp–bi gneiss	7.7	WJK21	qz–fsp–ms–bi gneiss	4.0
WJK212	qz–fsp–bi gneiss	8.9	WJK22	qz–fsp–ms–bi gneiss	5.3
WJK213	qz–fsp–bi gneiss	9.0	WJK23	qz–fsp–ms–bi gneiss	4.1
WJK214	qz–fsp–bi gneiss	9.0	WJK24	qz–fsp–ms–bi gneiss	6.3
WJK215	qz–fsp–bi schist	8.1	WJK36	qz–pl–ksp gneiss	7.7
WJK220	qz–pl–bi gneiss	7.9	WJK37	qz–bi–ep schist	6.8
			WJK50	qz–fsp–ms–bi gneiss	6.3
Tverregatelen			WJK68	qz–fsp–bi gneiss	10.5
WJK255	qz–bi–fsp gneiss	5.2	WJK74	qz–fsp–bi schist	4.2
WJK260	qz–bi–hbl–ep schist	4.7	WJK80	qz–ksp–pl–ms gneiss	9.3
WJK262	qz–fsp–ms gneiss	6.7	WJK82	qz–fsp–hbl–bi schist	6.3
WJK278	qz–ksp–ms–bi–pl–fl gneiss	8.1	WJK85	qz–fsp–bi schist	4.6
WJK282	qz–ksp–ms–bi–pl–fl gneiss	5.6	WJK95	qz–pl–bi schist	6.1
WJK283	qz mylonite	4.5	WJK97	qz–pl–bi schist	8.0
WJK285	qz–ksp–ms–bi–pl–fl gneiss	7.0	WJK99	qz–pl–bi–ep schist	2.9
WJK292	qz–ksp–ms–bi–pl–fl gneiss	10.0	WJK103	bi–qz–hbl–chlt schist	3.6
			WJK113	qz–bi–chl schist	1.7
Sistenup			WJK121	qz–fsp–bi pegmatite	9.6
WJK328	Tuff?	2.7	WJK123	qz–pl–bi gneiss	9.5
WJK329	Felsic lava	1.8			
WJK330	Felsic lava	3.5			
WJK336	Basalt	1.0			
WJK337	Plag–phyric basalt	−0.6 (plag −0.1)			
SIS5	Basalt	−1.8			
SIS8	Plag–phyric basalt	4.4 (plag 4.7)			
SIS48	Plag–phyric basalt	1.5			
SIS49	Basalt	0.7			
SIS51	Felsic lava	0.6			

Notes: qz, quartz; chl, chlorite; ksp, alkali feldspar; bi, biotite; pl, plagioclase; hbl, hornblende; ep, epidote. Samples WJK199–220 collected from vicinity of shearzone containing ultramylonite (WJK209).

Calc-silicate rocks

Calcite oxygen and carbon isotope data for the calc-silicate rocks are summarized in Table 2. Whole-rock samples of marble from the Fuglefjellet Formation at Skarsnuten range in $\delta^{18}O$ and $\delta^{13}C$ value from 13.3 to 26.8‰ and −2.4 to +2.8‰ respectively. The highest $\delta^{18}O$ and $\delta^{13}C$ values are from a homogeneous marble horizon (3 m thick; >90% sparry calcite). The samples with much lower $\delta^{18}O$ and $\delta^{13}C$ values were collected adjacent to intrusive undeformed pegmatite bodies of unknown age (WJS1 and 2), or from a calc-silicate boudin in the same area (WJS4).

The calcite from the calc-silicate boudins in the Kirwanveggen shows lower $\delta^{18}O$ (9.0 to 12.8‰) and much lower $\delta^{13}C$ (−7.4 to −11.1‰) values than the Skarsnuten marbles (Fig. 3).

Table 2. *Oxygen and carbon isotope data for carbonate rocks*

Sample	Location	$\delta^{18}O$ cc	$\delta^{13}C$ cc	$\delta^{18}O$ qz	wt.% cc
Boudins					
WJK81	Hall	10.0	−11.1		0.4
WJK83	Hall	9.6	−9.1		0.6
WJK145 B rim	Tva	10.4	−7.6		3.6
WJK145 C core	Tva	12.8	−7.4		51
WJK148	Tva	9.0	−8.6		4.3
Metasomatic					
CJK 96	Tvn	13.9	1.9		24
CJK 97	Tvn	11.4	2.9		41
CJK 98	Tvn	10.7	1.0		60
WJK269	Tvn	11.0	1.5		58
WJK270	Tvn	10.6	1.2		45
WJK271	Tvn	11.4	1.7		54
WJK 273 A vein	Tvn	12.6	−1.7		98
WJK 273 B boudin	Tvn	10.2	0.6		2.2
WJK 274 A	Tvn	13.4	0.9		20
WJK 274 B	Tvn	14.4	0.6		11
WJK 274 C	Tvn	13.5	0.9		32
WJK 274 D	Tvn	13.9	1.3		19
WJK 274 E	Tvn	14.9	2.6		83
WJK 274 F	Tvn	14.5	1.3		15
Fuglefjellet Formation					
WJS 1 contact with pegmatite	Skn	15.8	0.9		36
WJS 2 contact with pegmatite	Skn	13.3	−2.4	11.7	6.1
WJS 4 boudin	Skn	14.6	0.1	13.6	12
WJS 6 thick unit; cc-rich	Skn	26.8	2.8		81

Notes: cc, calcite; qz, quartz. Hall, Hallgrenskarvet; Tva, Tverrega; Tvn, Tverreggtelen; Skn, Skarsnuten.

A zoned boudin (WJK 145; Fig. 2a) consists of a calcite-rich core with $\delta^{13}C$ and $\delta^{18}O$ values of −7.4 and 12.8‰, respectively, and a silicate-rich outer zone with $\delta^{13}C$ and $\delta^{18}O$ values of −7.6 and 10.4‰, respectively. Similar values are seen in the other calc-silicate boudins.

The calcite from the late metasomatic body (Fig. 2b) shows a range in $\delta^{13}C$ and $\delta^{18}O$ values of −1.7 to 2.6‰ and 10.2‰ to 14.9‰ respectively (Fig. 3). Samples from the central zone have slightly higher $\delta^{18}O$ values than samples from the marginal zone. Sample WJK 274 consists of five generations of calc-silicate material (A, host calcite–amphibole–talc; B, coarse-grained amphibole–talc layer; C, calcite–amphibole–biotite layer; D, calcite boudin; E, a coarse calcite pod; and F, a single amphibole porphyroblast). The range in $\delta^{18}O$ value of all these components is 13.4 to 14.9‰ and the range in $\delta^{13}C$ values is from 0.6 to 2.6‰. Sample WJK273 from within the metasomatic body was taken from a boudin which contains a calcite-bearing vein. This sample has a similar $\delta^{18}O$ value (10.2‰) to the early calc-silicate boudins, but a much higher $\delta^{13}C$ value (0.6‰) which is similar to those of the metasomatic body.

Carbonate $\delta^{13}C$ and $\delta^{18}O$ values are plotted against wt.% calcite in Figure 3a, b. Apart from the core of one sample, the boudins contain <5 wt.% calcite (Table 2). The metacarbonate rocks from the Fuglefjellet Formation at Skarsnuten show reasonable positive correlations between both $\delta^{13}C$ and $\delta^{18}O$ values and wt.% calcite. The metasomatic carbonate rocks show no correlation between either $\delta^{13}C$ and $\delta^{18}O$ value and wt.% calcite.

Veins

The $\delta^{18}O$ values of quartz from the three different vein types (Fig. 2c–e) are presented in Table 3. There is a substantial range in vein quartz $\delta^{18}O$ values from 3.7 to 11.0‰, which is similar in magnitude to the range seen in the host rocks (1.7 to +10.5‰). The host rock $\delta^{18}O$ values show a positive correlation with those of the vein quartz (Fig. 4), with the majority of the veins having higher $\delta^{18}O$ values than the host rocks (average $\Delta_{vein-host} = 1.8‰$). A minority of veins, however have lower quartz $\delta^{18}O$ values than their immediate host rocks. Synfolial and

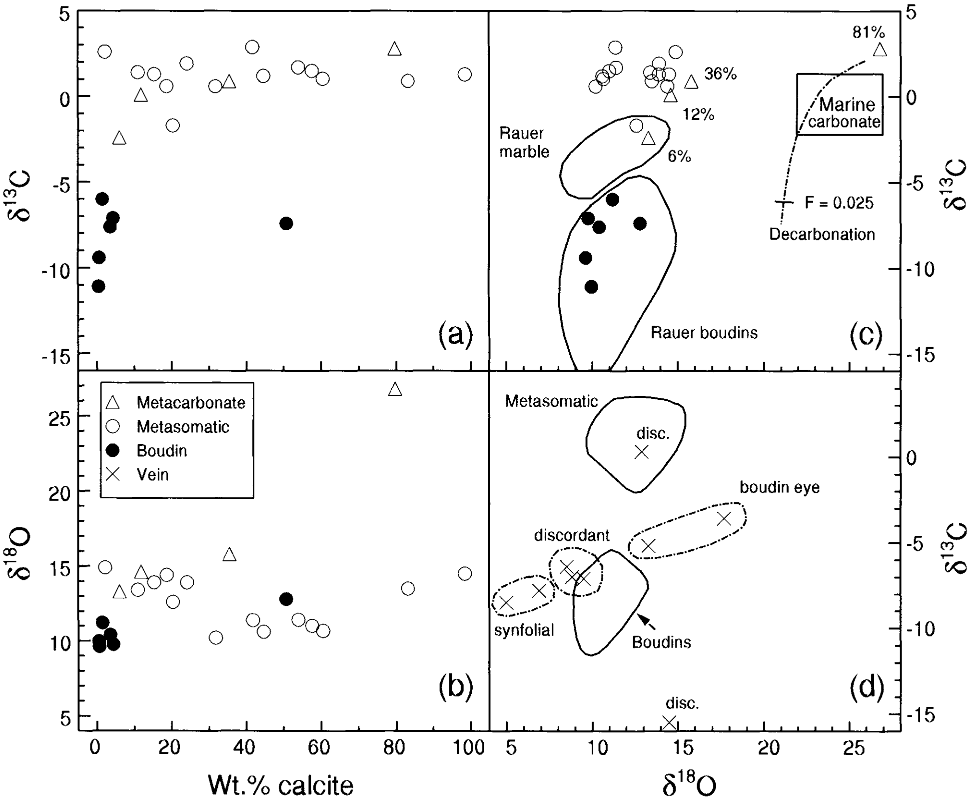

Fig. 3. Plot of $\delta^{13}C$ and $\delta^{18}O$ v. wt.% calcite (**a, b**) in the whole-rock for calc-silicate rocks from the central Kirwanveggen and the H.U. Sverdrupfjella. Plot of $\delta^{13}C$ v. $\delta^{18}O$ for calc-silicate (**c**) and calcite-bearing veins (**d**). The dashed curve in (**c**) is the path followed by an impure carbonate rock undergoing Rayleigh decarbonation starting from an arbitrary composition within the field for typical limestones assuming a $\alpha_{CO_2\ rock}$ of 1.0022 for C and a $\alpha_{CO_2\text{-}rock}$ of 1.012 for O. F (carbon), fraction of carbon remaining (Valley 1986). The fields for Rauer Group marbles and boudins (Buick *et al.* 1994) are shown as is a rectangle representing the typical values expected for marine carbonate (e.g. Viezer & Hoefs 1976). The types of veins are indicated on (**d**) where disc., discordant.

boudin-eye veins show a similar range in $\delta^{18}O$ values whereas the discordant veins (and their host rocks) tend to have higher $\delta^{18}O$ values (from 7.4 to 11.0‰).

In calcite-bearing quartz veins, the range in $\delta^{18}O$ values of the quartz is similar to that observed in all quartz veins (Fig. 4). The host-rock and vein quartz $\delta^{18}O$ values show a similar correlation to that seen in the quartz veins (Fig. 4). The calcite $\delta^{18}O$ values are much more variable than those of the quartz and with $\Delta_{quartz\text{-}calcite}$ ranging from 0.5 to −11.0‰. Apart from two samples, values of $\Delta_{quartz\text{-}calcite}$ are negative, whereas equilibrium fractionation between quartz and calcite should always be positive (e.g. Chiba *et al.* 1989). The correlation between vein calcite $\delta^{18}O$ and host rock $\delta^{13}C$ and $\delta^{18}O$ value is poor (Fig. 4). Synfolial calcite-bearing veins exhibit lower calcite $\delta^{18}O$ values than the boudin-eye veins whereas the discordant veins have intermediate calcite $\delta^{18}O$ values. Vein $\delta^{13}C$ v. $\delta^{18}O$ values are plotted on Figure 3d. Apart from two discordant veins, the samples show a good positive correlation but it is possible that this is an artefact of the small number of samples analysed.

Retrogressed rocks

Data from samples of banded gneiss, schist and other samples which show features of enhanced hydrous retrogression are presented in Table 1 and Figure 5. The range of $\delta^{18}O$ values for samples from Tverregga and Tverreggtelen is similar (4.9 to 12.0‰ and 4.5 to 10‰). Hallgrenskarvet

Table 3. *Oxygen and carbon isotope data for quartz and quartz–calcite veins*

Sample	Type	Location	$\delta^{18}O$ qz	$\delta^{18}O$ cc	$\delta^{13}C$ cc	Host rock	$\delta^{18}O$ wr
Quartz veins							
WJK4	synfolial	Hall	9.6			WJK3	8.5
WJK8	discordant	Hall	9.6			WJK1	7.8
WJK19	discordant	Hall	8.8			WJK15	8.3
WJK38	discordant	Hall	7.4			WJK37	6.8
WJK40	synfolial	Hall	7.5			WJK36	7.7
WJK56	synfolial	Hall	8.2			WJK55	6.8
WJK57	discordant	Hall	8.5			WJK55	6.8
WJK71	synfolial	Hall	9.2			WJK68	10.5
WJK75	synfolial	Hall	4.3			WJK74	4.2
WJK76	boudin eye	Hall	5.3			WJK74	4.2
WJK86	synfolial	Hall	6.7			WJK85	4.6
WJK87	boudin eye	Hall	5.8			WJK85	4.6
WJK96	synfolial	Hall	10.8			WJK97	8.0
WJK100	boudin eye	Hall	5.8			WJK99	2.9
WJK108	synfolial	Hall	6.6			WJK103	3.6
WJK111	boudin eye	Hall	8.5			WJK95	6.1
WJK122	boudin eye	Hall	10.4			WJK123	9.5
WJK164	synfolial	Tva	10.3			WJK159	8.7
WJK165	boudin eye	Tva	10.3			WJK159	8.7
WJK167	discordant	Tva	10.1			WJK160	9.3
WJK194	boudin eye	Tva	7.7			WJK193	4.9
WJK226	discordant	Tvn	9.9			WJK224	7.8
WJK244	synfolial	Tvn	8.1			WJK243	6.0
WJK257	synfolial	Tvn	7.9			WJK255	5.2
WJK261	synfolial	Tvn	6.9			WJK260	4.7
WJK263	synfolial	Tvn	7.8			WJK262	6.7
WJK279	synfolial	Tvn	6.7			WJK278	8.1
WJK283	synfolial	Tvn	4.5			WJK282	5.6
WJK286	discordant	Tvn	7.9			WJK285	7.0
WJK293	discordant	Tvn	9.2			WJK292	10.0
Calcite-bearing quartz veins							
WJK46	synfolial	Hall	5.2	5.0	−8.5	WJK44	2.5
WJK51	boudin eye	Hall	6.7	17.7	−3.6	WJK50	6.3
WJK79	discordant	Hall	11.0	14.5	−15.5	WJK80	9.3
WJK109	discordant	Hall	9.0	8.5	−6.4	WJK95	6.1
WJK110	discordant	Hall	8.8	9.5	−7.1	WJK95	6.1
WJK114	synfolial	Hall	3.7	6.9	−7.8	WJK113	1.7
WJK154	discordant	Tva	8.1	8.8	−7.0	WJK155	5.4
WJK166	boudin eye	Tva	10.8	13.3	−5.2	WJK159	8.7
WJK182	discordant	Tva	9.3	12.9	0.3	WJK180	10.4

Notes: cc, calcite; qz, quartz; wr, whole-rock. Hall, Hallgrenskarvet; Tva, Tverregga; Tvn, Tverreggtelen.

retrogressed rocks have generally lower $\delta^{18}O$ values with approximately one third of the samples having values <5.0‰. The lowest $\delta^{18}O$ value observed is 1.7‰ in a quartz–biotite–chlorite schist. Although the retrogressed rocks have generally lower $\delta^{18}O$ values than similar rock types not associated with the shear zones, there is no systematic change in $\delta^{18}O$ with distance across the shear zone. One of the mylonitic rocks from a high strain zone at Tverregga (WJK209) has slightly a higher $\delta^{18}O$ value (9.7‰) than the surrounding rocks, a similar mylonite at Tverregatelen has a much lower $\delta^{18}O$ value (4.5‰).

Discussion

The relationship between the materials analysed (Tables 1–3) and the metamorphic evolution of western Dronning Maud Land can be summarized as follows. Because the boudins are evidently associated with deformation, they must have formed during the Maud Orogeny (1200–900 Ma). Retrogression and rehydration during late fabric development in the central Kirwanveggen which appears to be associated with shear zones and the formation of mylonite are considered to be Cambrian in age, as is the

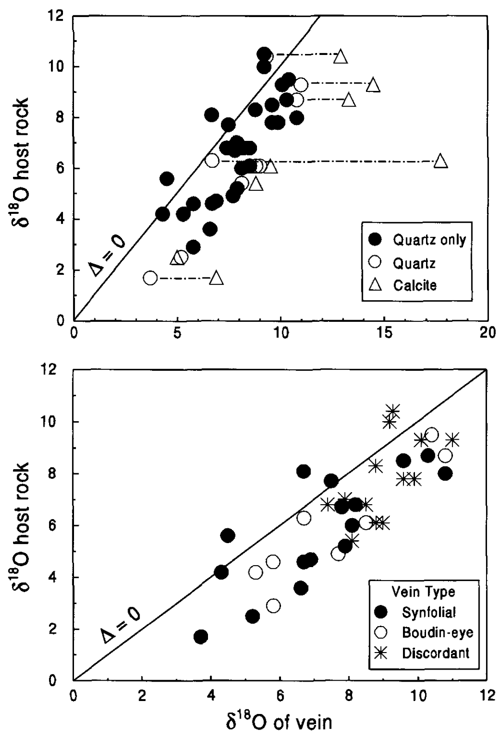

Fig. 4. Plot of quartz $\delta^{18}O$ (vein) v. whole-rock $\delta^{18}O$ (host) for veins from the central Kirwanveggen (lower diagram). The upper diagram compares the composition of quartz veins to quartz + calcite veins. Tie-lines join the compositions of coexisting quartz and calcite. The diagonal line indicates a value of $\Delta_{vein-host} = 0$ in both diagrams.

metasomatic calc-silicate body at Tverregtelen, which is associated with a shear zone. The lack of deformation of the Sistenup lavas means that the alteration must post-date the Maud Orogeny and for reasons discussed below, the alteration is most likely to be Cambrian in age. The veins possibly represent a wide range of ages. The boudin eye and synfolial veins are related to fabric development (see above) and must have formed during the Maud Orogeny, the discordant veins could have formed during either of the orogenic events.

Fluid–rock interaction during the Maud Orogeny

The calc silicate boudins in the Sverdrupfjella Group rocks have lower $\delta^{18}O$ and $\delta^{13}C$ values compared to the more massive metacarbonate samples from Skarsnuten (Fig. 3). Because the thick marble sequence is close to pure calcite (81%), decarbonation must have been limited and would not have had a significant effect on the carbon and oxygen isotope composition of this sample (WJS6, Table 2). The $\delta^{13}C$ value of WJS6 is slightly higher than normal for marine limestones, and it is possible that the original carbonate formed during a 'positive $\delta^{13}C$ excursion' (e.g. Viezer & Hoefs 1976). The other samples of Fuglefjellet marble plot on a curved path on Figure 3, with progressively lower $\delta^{18}O$ and $\delta^{13}C$ as the calcite content decreases. The Kirwanveggen boudins which, apart from the calcite-rich core of one sample, have <5 wt.% calcite lie on the extension of this curve. This type of curved path is typical for impure carbonate rocks which have undergone extensive decarbonation during metamorphism (e.g. Valley 1986). The theoretical decarbonation curve in Figure 3 represents Rayleigh decarbonation starting from the composition of the massive marble and assumes that the fluid was pure CO_2. If a mixed CO_2–H_2O fluid was present, H_2CO_3 would be more likely to be the dominant carbon-bearing species which has a smaller carbon isotope fractionation with calcite than CO_2 (e.g. Cartwright & Buick 1999), and the effects would be less pronounced.

Whereas the low $\delta^{13}C$ values and low calcite contents (<5 wt.%; Fig. 3a) of the boudins can be explained by decarbonation, it is clear that closed system decarbonation via loss of CO_2 cannot produce $\delta^{18}O$ values as low as those observed. The oxygen and carbon isotope patterns of these Kirwanveggen boudins are similar (Fig. 3) to those observed for zoned wollastonite–garnet boudins from the Rauer Group in East Antarctica (Buick *et al.* 1994). In the Rauer Group, fluid-flow is interpreted to be prior, and possibly unrelated to, peak metamorpism which was probably Cambrian in age (e.g. Sims & Wilson 1997). In the case of the Kirwanveggen, the calc-silicate bodies sampled were of the order of a few decimetres in size. Thus infiltration of fluid, which equilibrated isotopically at high-temperatures, with the surrounding silicate rocks (bulk rock $\delta^{18}O$ values typically between 7 and 10‰) could account for the low $\delta^{18}O$ values of the boudin calcite. The small volume of carbonate material relative to the surrounding silicates means that the fluid/rock ratio need not have been large, provided that the fluids were rock-buffered on a scale greater than the size of the boudins.

The synfolial and boudin eye quartz vein show a relatively good positive correlation between vein and host-rock $\delta^{18}O$ values, with an average difference between vein and host $\delta^{18}O$ value ($\Delta_{vein-host}$) of 1.8‰. The relationship between quartz vein and host rock $\delta^{18}O$ values can be used

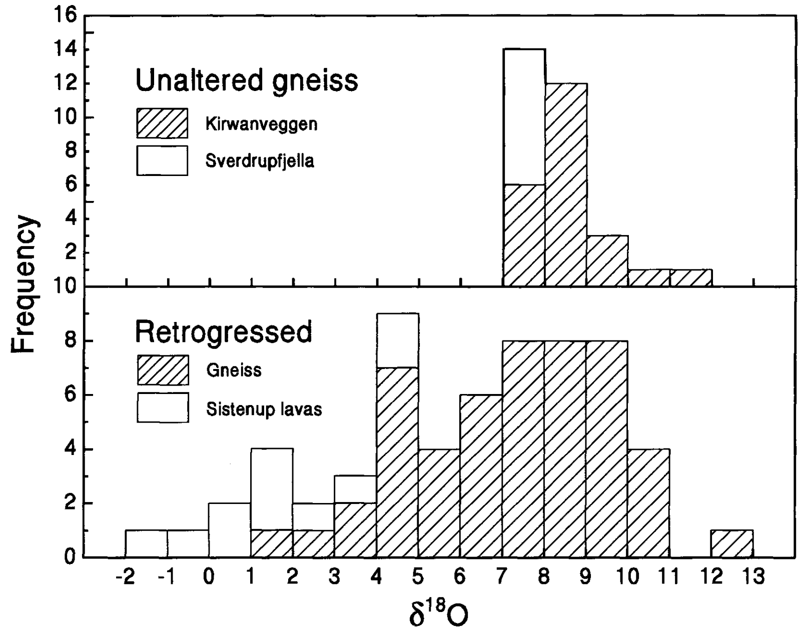

Fig. 5. Histogram showing the range of $\delta^{18}O$ values of retrogressed gneiss and schist samples, unretrogressed gneisses from the Kirwanveggen and H.U. Sverdrupfjella and the Sistenup lavas. Data from Table 3 (retrogressed rocks) and from Harris and Johnstone (unpublished data).

to distinguish between low fluid/rock ratio (rock-buffered) systems and those with greater relative volumes of fluid (fluid-buffered) (e.g. Gray *et al.* 1991; Henry *et al.* 1996). The synfolial and boudin eye vein/host relationship is generally consistent with rock-buffered conditions but samples where vein < host $\delta^{18}O$ value are more consistent with fluid-buffered conditions (Gray *et al.* 1991, p. 19 695). Consideration of only the synfolial quartz veins and their host rocks suggests that any lowering of $\delta^{18}O$ value, such as might have been experienced by the host rocks with $\delta^{18}O$ values, <*c.* 6‰ occurred during the early metamorphic history with synfolial quartz veins forming from fluids in oxygen isotope equilibrium with the host rocks.

The discordant veins are the youngest vein type analysed but are otherwise of uncertain age. They show a more restricted range of generally higher $\delta^{18}O$ values than the synfolial and boudin-eye veins and the data array on Figure 4 also suggests that they formed from fluids whose $\delta^{18}O$ values were generally rock-buffered. The relatively restricted range of $\delta^{18}O$ values is most likely a mineralogical effect in that only phyllosilicate-poor rocks (e.g. gneisses) were brittle enough to allow the formation of dicordant veins. Such rocks would have inherently higher $\delta^{18}O$ values because of the relatively large fractionation for oxygen between phyllosilicates and quartz/feldspar.

For veins containing both quartz and calcite, the quartz $\delta^{18}O$ value also correlates positively with the whole-rock $\delta^{18}O$ value. The co-existing calcite shows no correlation between its $\delta^{18}O$ value and that of the host and, as pointed out above, calcite $\delta^{18}O$ values are too high to be in equilibrium with the quartz (this applies to all three vein types; Fig. 4). Henry *et al.* (1996) reported similar disequilibrium between quartz and calcite in veins which they explained as being caused by later recrystallization of quartz during subsequent metamorphism. In the Kirwanveggen, the calcite has generally higher $\delta^{18}O$ values values than the quartz which suggests later equilibration (or precipitation) of calcite from lower temperature, possibly unrelated fluids.

^{18}O-depletion in the Sistenup lavas

The very low oxygen isotope ratios in the Sistenup lavas almost certainly resulted from the alteration episode that produced the groundmass amphibole, and are unlikely to be the original magmatic $\delta^{18}O$ values. Most unaltered basalts have $\delta^{18}O$ values >5.7‰ (Taylor & Sheppard 1987). A decrease in $\delta^{18}O$ value during metamorphism is normally interpreted (e.g. Valley 1986; Cartwright & Buick 1999) as indicating fluid–rock interaction at high fluid/rock ratios at high temperatures (>400°C). There are two possible causes of high temperature fluid–rock interaction at Sistenup. The lavas are exposed adjacent to a syenite intrusion which has been dated at 173 ± 2 Ma (Rb–Sr internal mineral isochron; Harris 1995). Fluid–rock interaction in the basalts could have occurred either as a result of hydrothermal activity associated with the intrusion of the syenite, or during regional metamorphism at some time prior to intrusion of the syenite. The latter explanation is favoured because:

(a) quartz and alkali feldspar within the syenite are in oxygen isotope equilibrium (Harris 1995), which is not consistent with circulation of an external fluid;
(b) although the whole-rock $\delta^{18}O$ values of the lavas are variable, they appear to be in internal oxygen isotope equilibrium ($\delta^{18}O$ plag $\sim \delta^{18}O$ whole-rock), which is not typical of hydrothermal aureoles (e.g. Forester & Taylor 1977); and
(c) the minerals within the syenite, even right at the contact, have $\delta^{18}O$ values consistent with equilibrium at magmatic temperatures, whereas lavas a few metres from the contact are highly depleted in ^{18}O.

The oxygen isotope fractionation factor between basalt and the altering fluid can be assumed to be approximately that of plagioclase (An_{50}) and water (that is 1.2‰ at 450°C and 0.3‰ at 600°C). If oxygen isotope equilibrium between the lavas and fluid were attained with the lava $\delta^{18}O$ values around zero, then the alteration fluid would have to have had a $\delta^{18}O$ value of −1.2‰, which is consistent with meteoric rather than magmatic water. It is suggested that the substantial fluid–rock interaction recorded at Sistenup is the result of a regional metamorphic/hydrothermal event post-dating the Maud Orogeny and pre-dating the intrusion of the Sistefjell syenite. This interpretation is supported by preliminary Ar–Ar dating of hornblende in the basalt (D. Phillips, pers. comm., 2000). Given the lack of deformation, the alteration is likely to be Cambrian in age.

Cambrian fluid–rock interaction in the Sverdrupfella Group

Calcite from the metasomatic calc silicate body has $\delta^{18}O$ values between 9 and 15‰ and is consistent with the oxygen isotope composition being buffered by the surrounding silicate assemblages. The $\delta^{13}C$ values are similar to those of the metacarbonates of the Fuglefjellet Formation which may have been the source of carbon in the fluid responsible for the metasomatism. These rocks are the only volumetrically important carbonate rocks exposed in the area and are situated some 150 km NE of the central Kirwanveggen. If the Fuglefjellet rocks are the source of carbon this implies regional-scale movement of fluids.

Petrographical evidence for hydrous retrogression in rocks associated with high strain zones indicates possible infiltration of fluids via these late structural features which are considered to be early Cambrian in age (Grantham *et al.* 1995; Johnstone *et al.* 1998; Jackson 1999). The $\delta^{18}O$ values of the retrogressed rocks are compared with samples of unaltered gneiss in Figure 5. The retrogressed rocks show a negative skewed distribution, with the main peak at the same values as the unaltered gneisses, but with a significant number of rocks having much lower $\delta^{18}O$ values. In part this might be due to the mineralogy of the materials analysed. The gneisses samples are generally leucocratic and are dominated by quartz and feldspar, minerals that concentrate ^{18}O, whereas some of the retrogressed samples are rich in biotite, and/or amphibole, and/or chlorite which would lead to lower $\delta^{18}O$ values even in assemblages in equilibrium with the gneisses. Although in some rocks mineralogical effects do appear to be the cause of 'low' $\delta^{18}O$, a significant proportion of samples with $\delta^{18}O <$ 6‰ are quartz–feldspar dominated gneisses (Table 1). Felsic gneiss samples with the low $\delta^{18}O$ values indicate exchange with external fluids which themselves have a low $\delta^{18}O$ value (meteoric water), as discussed above for the Sistenup lavas. None of the retrogressed samples, however, has as low $\delta^{18}O$ values as the Sistenup lavas (with the lowest $\delta^{18}O$ values) and the lack of systematic shifts in $\delta^{18}O$ value across the high-strain zones indicates relatively limited influx of such fluids.

Conclusions

The nature of the Cambrian overprinting in western Dronning Maud Land is poorly understood. Regional resetting of the Rb–Sr, Sm–Nd and K–Ar systems in the area (Moyes *et al.* 1993) suggests more than the passive thermal effects associated with the intrusion of a limited volume of 460–500 Ma granitoids. The stable isotope data presented in this paper documented multiple episodes of fluid–rock interaction. The calc-silicate boudins in the Sverdrupfjella Group record fluid–rock interaction between 1200 and 900 Ma during the Maud Orogeny. Various generations of quartz and quartz–calcite veins appear to have formed from fluids whose isotope compositions were largely rock-buffered with low fluid/rock ratios. Extensive fluid–rock interaction with externally derived fluids are required by the very low $\delta^{18}O$ values of the Sistenup lavas. Their lack of deformation indicates that ^{18}O-depletion occurred during the Cambrian. The high-strain zones are the features in the Sverdrupfjella group most likely to be related to early Cambrian metamorphism. A significant number of samples from within and adjacent to high strain zones that show petrographical evidence of hydrous retrogression exhibit ^{18}O-depletion, which requires interaction with externally derived fluids. Although the ^{18}O-depletion in the high-strain zones was not to the same extent as seen at Sistenup, it is suggested that the two events are related. Also associated with a late shear zone is the metasomatic calc-silicate body at Tverreggtelen in the central Kirwanveggen. This body shows very different carbon isotope character to the calc-silicate boudins in nearby nunataks. The overlap in $\delta^{13}C$ values between this body and the Fuglefjellet 150 km to the NE suggests a possible source of carbon and movement of fluids on a regional scale. Granitic plutons of Cambrian age are present in the H.U. Sverdrupfella (Grantham *et al.* 1995; Groenewald *et al.* 1995) and are more abundant further east (e.g. Shiraishi *et al.* 1992). It is suggested that these intrusions provided the driving mechanism for infiltration of dominantly meteoric fluids along high-strain zones.

The authors would like to thank Warwick Board and Branko Corner for their contributions to this research. We greatly appreciate the contribution of Chris Jackson who read and commented on an earlier version of this paper and provided some of the samples used in this study. Most of the analyses were done by Fayrooza Rawoot at the University of Cape Town and we thank Ian Cartwright and Marlen Yanni of Monash University for additional analyses. Ian Buick, Ian Cartwright and Jodie Miller provided comments which helped to improve the manuscript substantially. This study was funded by the South African National Antarctic Programme.

References

APTED, M. J. & LIOU, J. G. 1983. Phase relations among greenschist, epidote–amphibolite, and amphibolite in a basaltic system. *American Journal of Science*, **283-A**, 328–354.

BORTHWICK, J. & HARMON, R. S. 1982. A note regarding ClF_3 as an alternative to BrF_5 for oxygen isotope analysis. *Geochemica et Cosmochemica Acta*, **46**, 1665–1668.

BUICK, I. S., HARLEY, S. L., CARTWRIGHT, I. & MATTEY, D. 1994. Stable isotopic signatures of superposed fluid events in granulite-facies marbles of the Rauer Group, East Antarctica. *Journal of Metamorphic Geology*, **12**, 285–299.

CARTWRIGHT, I. & BUICK, I. S. 1999. The flow of surface-derived fluids through Alice Springs age middle-crustal ductile shear zones, Reynolds Range, central Australia. *Journal of Metamorphic Geology*, **17**, 397–414.

CHIBA, H., CHACKO, T., CLAYTON, R. N. & GOLDSMITH, J. R. 1989 Oxygen isotope fractionations involving diopside, forsterite, magnetite, and calcite: applications to geothermometry. *Geochimica et Cosmochimica Acta*, **53**, 2985–2995.

COPLEN, T. B., KENDALL, C. & HOPPLE, J. 1983. Comparison of stable isotope reference samples. *Nature*, **302**, 236–238.

CORNER, B. 1994. *Geophysics Report*. Final project report, South African National Antarctic Programme, Pretoria.

DIRKS, P. H. G. M., CARSON, C. J. & WILSON, C. J. L. 1993. The deformational history of the Larsemann Hills, Prydz Bay: the importance of the Pan-African (500 Ma) in East Antartica. *Antarctic Science*, **5**, 179–192.

FORSETER, R. W. & TAYLOR, H. P. 1977. $^{18}O/^{16}O$ D/H and $^{13}C/^{12}C$ studies of the tertiary igneous complex of Skye, Scotland. *American Journal of Science*, **277**, 136–177.

FITZSIMONS, I. C. W. 1998. Early Cambrian tectonism in East Antarctica: implications for Gondwana assembly and earlier supercontinents. Special abstracts issue Gondwana 10: Event stratigraphy of Gondwana. *Journal of African Earth Sciences*, **27**, 74–75.

GRANTHAM, G. H., JACKSON, C., MOYES, A. B., GROENEWALD, P. B., HARRIS, P. D., FERRAR, G. & KRYNAUW, J. R. 1995. The tectonothermal evolution of the Kirwanveggen–H.U. Sverdrupfjella areas, Dronning Maud Land, Antarctica. *Precambrian Research*, **75**, 209–229.

GRAY, D. R, GREGORY, R. T. & DURNEY, D. W. 1991. Rock-buffered fluid-rock interaction in deformed quartz-rich turbidite sequences, eastern Australia. *Journal of Geophysical Research*, **96** 19 681–19 704.

GROENEWALD, P. B. 1991. Metamorphic evolution of the, H.U. Sverdrupfjella in the context of Maudheim orogenic province, western Dronning Maud Land, Antarctica. *In*: *6th International Symposium on Antarctic Earth Sciences*. NIPR, Tokyo.

GROENEWALD, P. B., MOYES, A. B., GRANTHAM, G. H. & KRYNAUW, J. R. 1995. East Antarctic crustal evolution: geological constraints and modeling in western Dronning Maud Land. *Precambrian Research*, **75**, 231 250.

HARRIS, C. 1995. *Petrogenesis of the Sistefjell syenite complex, Dronning Maud land, Antarctica: generation of low $\delta^{18}O$ magmas by contamination of rift zone magmas*. Abstract Volume, Centennial Geocongress, Johannesburg, 235–239.

HARRIS, C. & ERLANK, A. J. 1992. The production of large volume low-$\delta^{18}O$ rhyolites during the rifting of Africa and Antarctica: The Lebombo monocline, southern Africa. *Geochemica et Cosmochimica Acta*, **56**, 3561–3570.

HENRY, C., BURKHARD, M. & GOFFÉ, B. 1996. Evolution of synmetamorphic veins and their wallrocks through a Western Alps transect: no evidence for large-scale fluid-flow. Stable isotope, major and trace-element systematics. *Chemical Geology* **127**, 81–109.

HJELLE, A. 1974. Some observations on the geology of the, H.U. Sverdrupfjella, Dronning Maud Land, Antarctica. *Arbor 1972*, **7–22**. Norsk Polarinstitutt, Oslo, Norway.

JACKSON, C. 1999. *Characterization of Mesoproterozoic to Palaeozoic crustal evolution of Western Dronning Maud Land.* Final project report, South African National Antarctic Programme.

JOHNSTONE, W. P., HARRIS, C. & JACKSON, C. 1998. Fluid-rock interaction related to deformation and regional metamorphism of the circum East Antarctic Mobile Belt in western Dronning Maud Land, Antarctica. Special abstracts issue Gondwana 10: Event stratigraphy of Gondwana. *Journal of African Earth Sciences*, **27**, 122–123.

KRYNAUW, J. R. 1996. A Review of the Geology of East Antarctica, with special Reference to the *c.* 1000 Ma and *c.* 500 Ma Events. *Terra Antarctica*, **3**(2), 77–89.

MCCREA, J. M. 1950. On the isotopic chemistry of carbonates and a paleotemperature scale. *Journal of Chemical Physics*, **18**, 849–857.

MOODY, J. B., MEYER, D. & JENKINS, J. E. 1983. Experimental characterization of the greenschist/amphibolite boundary in mafic systems. *American Journal of Science*, **283**, 48–92.

MOYES, A. B., BARTON, J. M. & GROENEWALD, P. B. 1993. Late Proterozoic to early Palaeozoic tectonism in Dronning Maud Land, Antarctica: its bearing on supercontinental fragmentation and amalgamation. *Journal of the Geological Society, London*, **150**, 833–842.

PILI, E., SHEPPARD, S. M. F., LARDEAUX, J.-M., MARTELAT, J.-M. & NICOLLET, C. 1997. Fluid flow vs. scale of shear zones in the lower continental crust and the granulite paradox. *Geology*, **25**, 15–18.

RAVICH, M. G. & SOLOV'EV, D. S. 1969. *Geology and petrology of the mountains of central Queen Maud Land.* Israel Programme for Scientific Translations, Jerusalem.

ROOTS, E. F. 1969. *Geology of western Dronning Maud Land.* Explanation of Plate VI, Folio **12**, Antarctic Map Series, American Geophysical Union.

SIMS, J. P. & WILSON, C. J. L. 1997. Strain localisation and texture development in a granulite-facies shear zone – the Rauer Group, East Antarctica. *In*: RICCI, C. A. (ed.) *The Antarctic Region: Geological Evolution and Processes*. Terra Antarctica, Siena, Italy, 131–138.

SHIRAISHI, K., HIROI, Y., ELLIS, D. J., FANNING, C. M., MOTOYOSHI, Y. & NAKAI, Y. 1992. The first report of a Cambrian orogenic belt in East Antarctica – an ion microprobe study of Lutzow-Holm complex. *In*: YOSHIDA, Y., KAMINUMA, K. & SHIRAISHI, K. (eds) *Recent progress in Antarctic Earth Science*. Terrapub, Toyko, 29–36.

TAYLOR, H. P. & SHEPPARD, S. M. F. 1987. Igneous rocks I. Processes of isotopic fractionation and isotope systematics. *In*: VALLEY, J. W., TAYLOR, H. P. & O'NEIL, J. R. (eds) *Stable Isotopes in High Temperature Geological Processes*. Reviews in Mineralogy, **16**, 227–271.

VALLEY, J. W. 1986. Stable isotope geochemistry of metamorphic rocks. *In*: VALLEY, J. W., TAYLOR, H. P. & O'NEIL, J. R. (eds) *Stable Isotopes in High Temperature Geological Processes*. Reviews in Mineralogy, **16**, 445–490.

VENNEMANN, T. W. & SMITH, H. S. 1990. The rate and temperature of reaction of ClF_3 with silicate minerals, and their relevance to oxygen isotope analysis. *Chemical Geology*, **86**, 83–88.

VIEZER, J. & HOEFS, J. 1976. The nature of $^{18}O/^{16}O$ and $^{13}C/^{12}C$ secular trends in sedimentary carbonate rocks. *Geochimica et Cosmochimica Acta*, **40**, 1387–1395.

WOLMARANS, L. G. & KENT, K. E. 1982. Geological investigations in western Dronning Maud Land, Antarctica – a synthesis. *South African Journal of Antarctic Research*, **2**, 93.

YOSHIDA, M. 1992. Late Proterozoic to Early Palaeozoic events in East Gondwanian crustal fragments. *In*: *29th International Geological Congress*, Abstracts. Kyoto, **2/3**, 265.